An Automated Image-Based Tool for Pupil Plane Characterization of EUVL Tools

Zac Levinson[a], Jack S. Smith[a], Germain Fenger[b], Bruce W. Smith[a]

[a]Rochester Institute of Technology, 168 Lomb Memorial Drive, Rochester, NY 14623
[b]Mentor Graphics, Kapeldreef 75, 3001 Heverlee, Belgium

ABSTRACT

Pupil plane characterization will play a critical role in image process optimization for EUV lithography (EUVL), as it has for several lithography generations. In EUVL systems there is additional importance placed on understanding the ways that thermally-induced system drift affect pupil variation during operation. In-situ full pupil characterization is therefore essential for these tools. To this end we have developed Quick Inverse Pupil (QUIP)—a software suite developed for rapid characterization of pupil plane behavior based on images formed by that system. The software consists of three main components: 1) an image viewer, 2) the model builder, and 3) the wavefront analyzer. The image viewer analyzes CD-SEM micrographs or actinic mask micrographs to measure either CDs or through-focus intensity volumes. The software is capable of rotation correction and image registration with subpixel accuracy. The second component pre-builds a model for a particular imaging system to enable rapid pupil characterization. Finally, the third component analyzes the results from the image viewer and uses the optional pre-built model for inverse solutions of pupil plane behavior. Both pupil amplitude and phase variation can be extracted using this software. Inverse solutions are obtained through a model based algorithm which is built on top of commercial rigorous full-vector simulation software.

Keywords: EUV lithography, EUV aberrations, aberration metrology, image-based aberration metrology, pupil characterization

INTRODUCTION

Pupil plane characterization and manipulation have played a critical role in image-process optimization of past technology nodes.[1–3] The criticality of pupil characterization continues into EUV lithography (EUVL) with an additional importance placed on understanding the ways that the pupil variation evolves during system operation.[4,5] Interferometric techniques are the de-facto standard of wavefront analysis. These techniques have been demonstrated with sub-nanometer resolution but require the use of additional optics, and are therefore difficult to implement during system use.[6–8] In addition, we have previously shown that amplitude pupil variation in EUV imaging systems can be non-uniform.[9]

We have developed Quick Inverse Pupil (QUIP)—a software suite developed for rapid characterization of pupil plane behavior based on images formed by that system. Both pupil amplitude and phase variation can be extracted using this software. Inverse solutions are obtained through a model based algorithm which is built on top of commercial rigorous full-vector simulation software. In the past we have presented an iterative technique to extract the phase and amplitude pupil variation of an EUVL system from images formed by that system.[10–13] We have demonstrated this technique on several EUV optical systems.[11,9,13] In addition, we have developed a new algorithm based on principal component analysis (PCA). Although this results in a potentially lengthy model building step, the wavefront analysis step can be completed in under a quarter second. Model building only needs to be completed once for each imaging system.

QUIP consists of three main components: 1) an image viewer, 2) the model builder, and 3) the wavefront analyzer. Each of these components has been designed for ease of use. Minimal knowledge of the lithography process and no knowledge of process simulation is necessary for operation of the software. In this paper we will examine the algorithms and features in each of the components in the QUIP software suite.

Extreme Ultraviolet (EUV) Lithography VII, edited by Eric M. Panning, Proc. of SPIE Vol. 9776,
97762M · © 2015 SPIE · CCC code: 0277-786X/15/$18 · doi: 10.1117/12.2219704

Downloaded From: http://proceedings.spiedigitallibrary.org/ on 03/24/2016 Terms of Use: http://spiedigitallibrary.org/ss/TermsOfUse.aspx

THEORY

The transfer of light through an optical system can be represented by its pupil function, which is in general complex valued and can therefore be represented in terms of its amplitude and phase.[14,15] It is customary to expand the phase function in a Fourier-Zernike series as[15,16],

$$W(u,v) = \sum_{n=0}^{\infty} a_n Z_n(\rho,\phi) \tag{1}$$

Where (ρ,ϕ) represents polar coordinates defined in terms of normalized frequency coordinates, (u,v), and Z_n represents the nth Zernike polynomial.[16,17] We have shown the amplitude is not uniform across the pupil, as is traditionally assumed, in EUVL systems. Therefore, we redefine the amplitude function in terms of a separate Fourier-Zernike series given as,

$$\alpha(u,v) = 1 + \sum_{n=0}^{\infty} b_n Z_n(\rho,\phi) \tag{2}$$

We have identified a number of pattern types, already present on most masks, which are sensitive to specific types of Zernike polynomials, as shown in Figure 1a. If a certain aberration is present, then there will be a phase or amplitude difference between the measurement sites of these targets.[13] The pupil variation of an optical system can then be extracted via the images of these targets as in the algorithm described by Figure 1b.

To begin, we assume that the system is aberration free. A model is constructed between the explanatory variables and the CD difference via aerial image simulations. Experimental data (either aerial image or CD data) can can then be fit to this model to obtain an initial guess for that particular aberration. Finally, the process repeats until the algorithm converges on a solution for the pupil variation. This technique is presented in more detail in our previous report.[13]

Alternatively, a model can be pre-computed using an algorithm based on principal component analysis (PCA). This process is detailed graphically in Figure 1c. Using this algorithm, a set of 1D aerial images through-focus (*intensity volume*) is simulated corresponding to a full factorial experiment and this dataset is analyzed using PCA. Then a model is constructed between the treatment combinations and the results of PCA. This model can be easily inverted when experimental data is obtained. This technique is presented in more detail in a previous paper.[18]

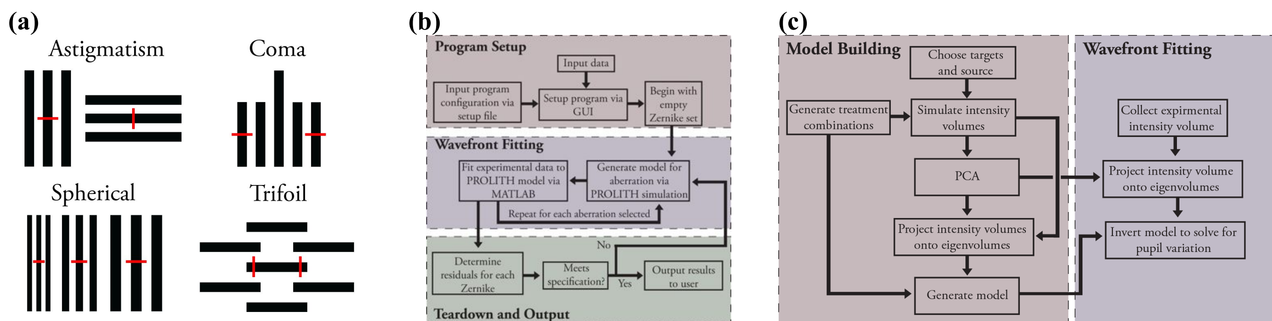

Figure 1. (a) Examples of metrology targets for each primary aberration. The red lines denote measurement locations. The aberration is interrogated by the CD difference at measurement sites. (b) A flowchart for the iterative algorithm of image-based pupil characterization. (c) A flowchart for the PCA-based algorithm of image-based pupil characterization.

The PCA-based algorithm separates the model building and wavefront analysis steps into two distinct stages. While it may take tens of hours to build the models this only needs to be completed once. Afterwards the wavefront can be extracted from experimental data in less than a quarter second. Presently this algorithm requires approximate through-focus aerial images, which we call an intensity volume. CD can still be used in QUIP, but the iterative algorithm must be used instead.

Downloaded From: http://proceedings.spiedigitallibrary.org/ on 03/24/2016 Terms of Use: http://spiedigitallibrary.org/ss/TermsOfUse.aspx

IMAGE VIEWER

The first step to wavefront analysis in QUIP is to use the image viewer to extract the necessary image data. The software can read CD-SEM and scanner lot reports to automatically link this data to image measurements. The image viewer interface in shown in Figure 2. To begin, either CD-SEM micrographs or through focus image stacks are loaded into the software. Stage errors can be corrected through subpixel image rotation and registration algorithms. If necessary, noise can be filtered from the image and, finally, a region of interest is selected and optionally interpolated. The CD or through-focus intensity volume can then be extracted from this region.

In CD-SEM micrographs there is often a large amount of high frequency noise originating from secondary electron noise. This type of noise affects CD measurements but can be filtered by using either a median filter or a Savitzky-Golay filter. An example of unfiltered vs. median filtered image is given in Figure 3a. The effect of the filter is more easily seen when comparing intensity line scans between the two images, Figure 3b.

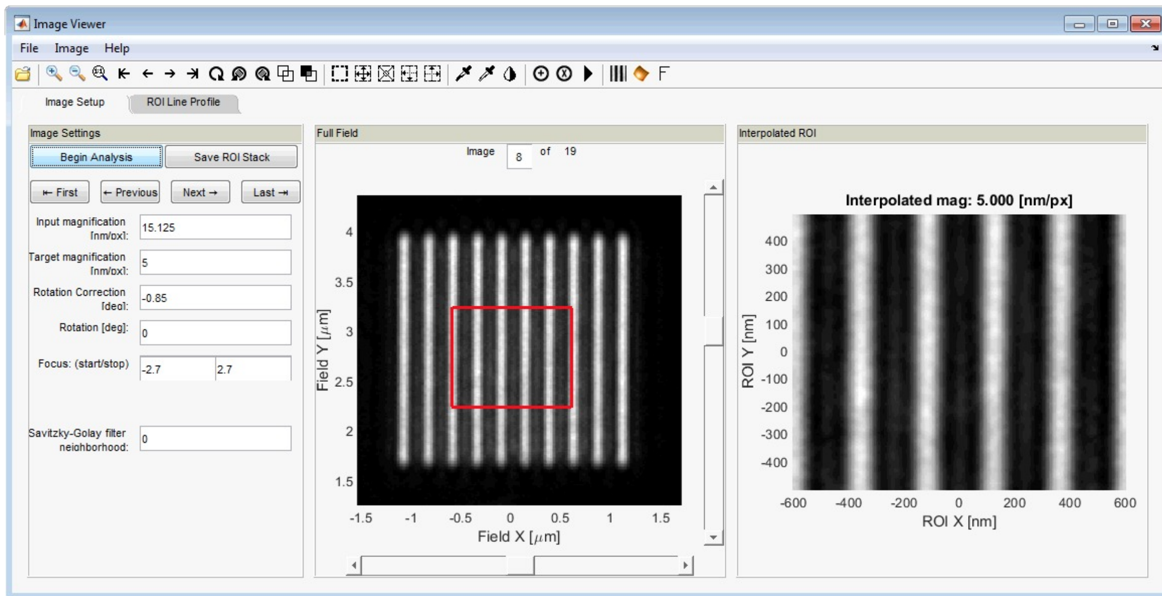

Figure 2. The Image Viewer interface showing a sample image from an EUV actinic mask microscope.

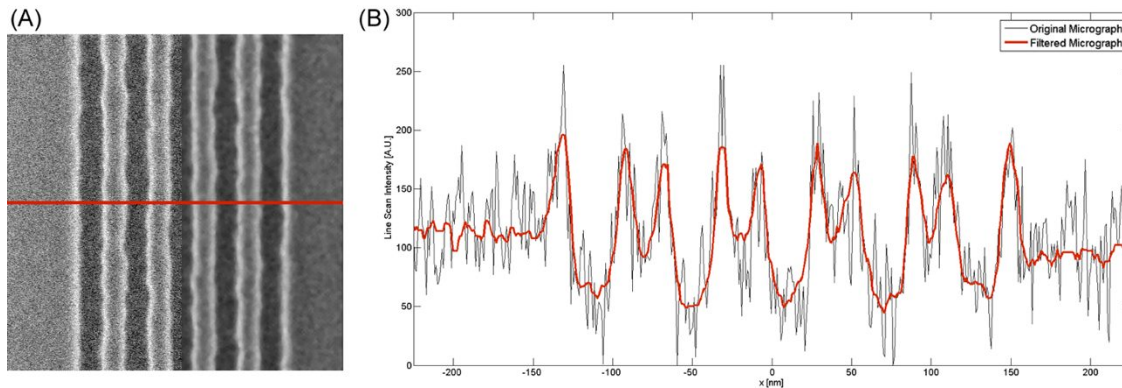

Figure 3. Example of SEM micrograph image processing for NXE:3100 case study. a) A comparison of the original (left) and median filtered (right) images, b) plot of a intensity line scan across the line in part (a) for both the original and filtered images.

Downloaded From: http://proceedings.spiedigitallibrary.org/ on 03/24/2016 Terms of Use: http://spiedigitallibrary.org/ss/TermsOfUse.aspx

Rotation correction is computed by selecting an edge which should be straight. The software can then determine the appropriate offset to correct the rotation of this edge. Other stage errors can be corrected through the registration of the image stack. Image translation is determined with subpixel accuracy via the frequency domain phase of the cross-correlation of adjacent images.[19] Next, the image can be interpolated to a higher pixel grid, which also deconvolves the response of the CCD sensor. This process is shown in Figure 4a, where an image collected at approximately 15 nm/px was interpolated to approximately 5 nm/px. Finally, the aerial image or SEM line scan can be approximated via the normalized column-wise median of the interpolated region. The CD can then be measured by thresholding the profile, or the through-focus intensity volume can be captured by saving the profile from a through-focus image stack.

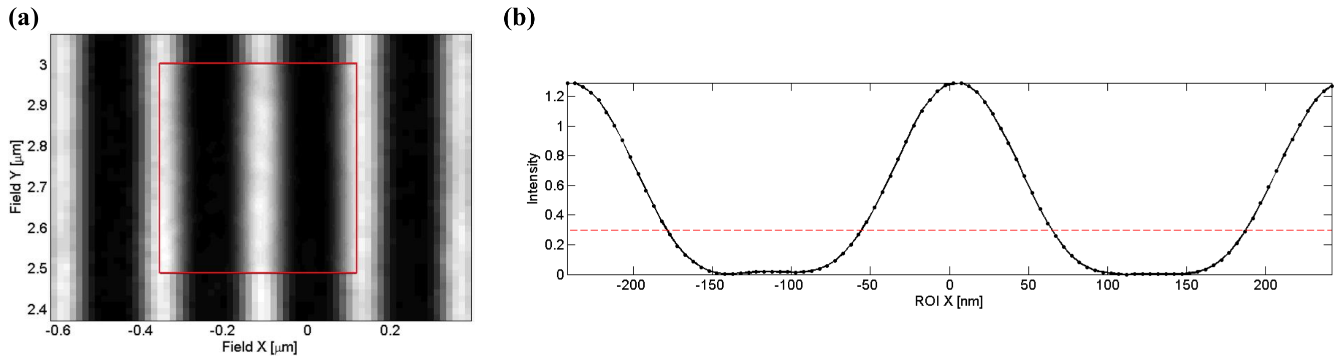

Figure 4. (a) An example image at the original resolution and after Fourier interpolation (inset). (b) Column-wise average of the interpolated region in the inset of panel (a) to estimate the aerial image.

MODEL BUILDER

The next step in wavefront analysis in QUIP is to pre-build a model if the PCA-based algorithm is to be used. The Model Builder interface is shown in Figure 5. The software assists in setting up and running the aerial image simulations necessary to build the desired models. Response variables can be amplitude and/or phase pupil variation specified by Zernike polynomials. An optional setup file can be used to specify the default values of the interface.

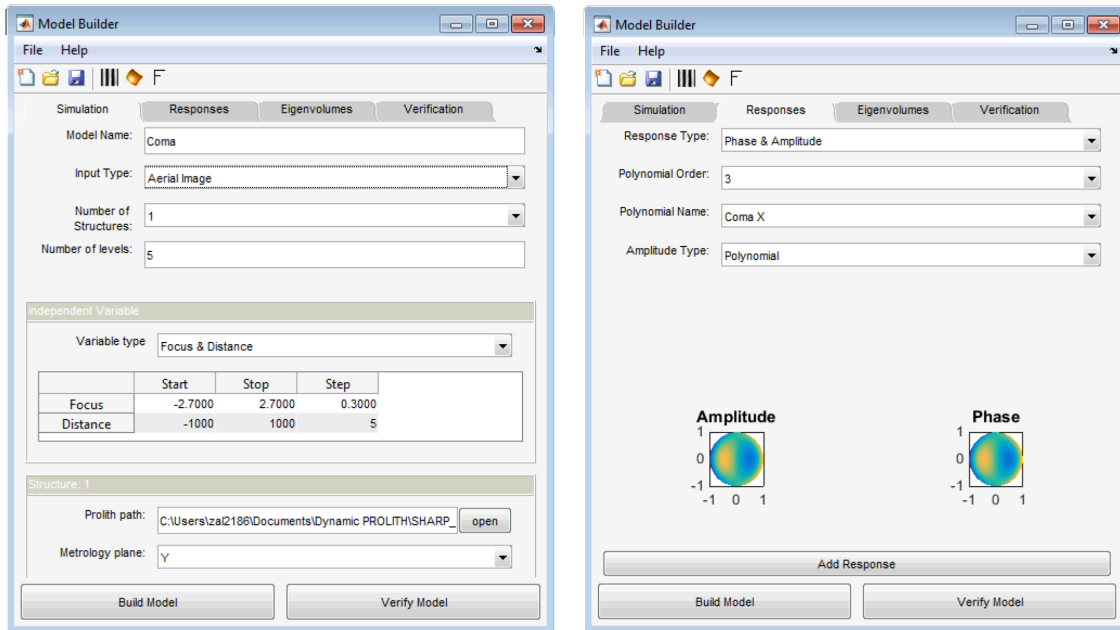

Figure 5. The Model Builder interface showing the setup for a sample model to interrogate Z_7 amplitude and phase pupil variation. The left shows the setup for the aerial image simulations, while the right shows choosing the response variables for the model.

Downloaded From: http://proceedings.spiedigitallibrary.org/ on 03/24/2016 Terms of Use: http://spiedigitallibrary.org/ss/TermsOfUse.aspx

After running the appropriate simulations, the eigenvolumes obtained via PCA can be viewed directly in the software. The eigenvolume shows the aerial image variation caused by a certain aberration. A polynomial model is constructed between the simulated treatment combinations and projections of intensity volumes onto the selected eigenvolumes. The appropriate order of the polynomial can be determined via Akaike information criterion. This is an information theoretic approach to quantifying over-fitting risk, and is built in directly to the software. The RMSE of the models is also computed to quantify the robustness of the models.

WAVEFRONT ANALYZER

The final step in wavefront analysis in QUIP is to use the wavefront analyzer. The interface of this component is shown in Figure 6. Like the Model Builder, an optional setup file can be used to specify defaults values. If a model has been pre-built in the Model Builder, then this can be loaded into the software and an inverse pupil solution can be obtained rapidly by loading the corresponding experimental data. If the iterative algorithm is to be used, then the appropriate simulations must be set up at this point. Regardless of algorithm, the results of the analysis are output both numerically and graphically. In addition, the results may be save to a CSV file.

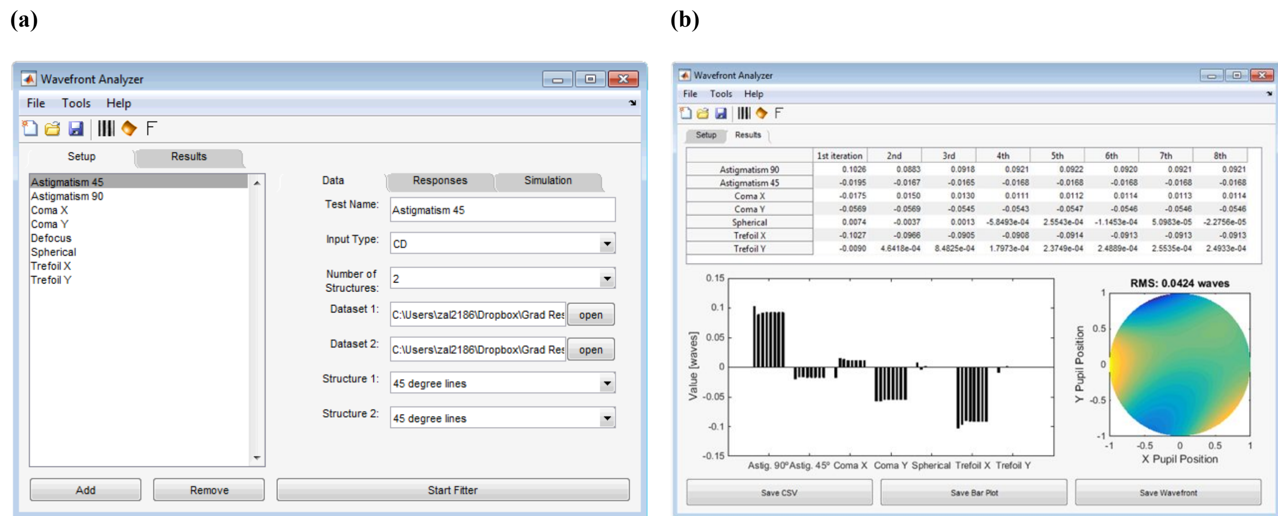

Figure 6. (a) The Wavefront Analyzer interface showing a sample setup to interrogate the primary phase aberrations. (b) The Wavefront Analyzer showing the results running the setup shown in panel (a) using the iterative algorithm.

CONCLUDING REMARKS

We are developing a software suite to provide image-based in situ pupil monitoring for EUV systems. Quick Inverse Pupil (QUIP) enables rapid characterization of both pupil amplitude and phase variation. The software is split into three separate software components, which facilitate easy pupil characterization. Both CD data and through-focus intensity data can be used for inverse solutions. The software offers two separate wavefront analysis algorithms: an iterative procedure and an algorithm based on principal component analysis. At the moment the PCA-based algorithm only supports through-focus intensity data. Using this algorithm inverse solutions can be obtained in less than a quarter second. While the iterative algorithm is slower, it can be used with both types of image data.

ACKNOWLEDGEMENTS

The authors would like to thank KLA Tencor for use of the PROLITH™ lithography simulator.

Downloaded From: http://proceedings.spiedigitallibrary.org/ on 03/24/2016 Terms of Use: http://spiedigitallibrary.org/ss/TermsOfUse.aspx

REFERENCES

[1] Kempsell Sears, M., Fenger, G., Mailfert, J.., Smith, B., "Extending SMO into the lens pupil domain," Proc. SPIE 7973, 79731B – 79731B – 9 (2011).

[2] Kempsell Sears, M., Bekaert, J.., Smith, B. W., "Pupil wavefront manipulation for optical nanolithography," Proc. SPIE 8326, 832611–832611 – 11 (2012).

[3] Baylav, B., Maloney, C., Levinson, Z., Bekaert, J., Vaglio Pret, A.., Smith, B. W., "Impact of pupil plane filtering on mask roughness transfer," J. Vac. Sci. Technol. B Microelectron. Nanometer Struct. **31**(6), 06F801 (2013).

[4] Bakshi, V., [EUV Lithography], SPIE, 1000 20th Street, Bellingham, WA 98227-0010 USA (2008).

[5] Krautschik, C. G., Ito, M., Nishiyama, I.., Mori, T., "Quantifying EUV imaging tolerances for the 70-, 50-, 35-nm modes through rigorous aerial image simulations," Proc. SPIE 4343, 524–534 (2001).

[6] Foucault, L., "Description des procedees employes pour reconnaitre la configuration des surfaces optiques," C R Acad Sci 47, 958ff (1858).

[7] Linnik, W. P., "A simple interferometer for the investigation of optical systems," Proc Acad. Sci USSR **1**, 208 (1933).

[8] Naulleau, P. P., Goldberg, K. A.., Bokor, J., "Extreme ultraviolet carrier-frequency shearing interferometry of a lithographic four-mirror optical system," J. Vac. Sci. Technol. B **18**(6), 2939–2943 (2000).

[9] Levinson, Z., Verduijn, E., Wood, O. R., Mangat, P., Goldberg, K. A., Benk, B. Markus P., Wojdyla, A.., Smith, B. W., "Measurement of EUVL Pupil Amplitude and Phase Variation via Image-Based Methodology," *In Preparation* (2016).

[10] Zavyalova, L. V., Smith, B. W., Suganaga, T., Matsuura, S., Itani, T.., Cashmore, J. S., "In-situ aberration monitoring using phase wheel targets," Proc. SPIE 5377, 172–184 (2004).

[11] Levinson, Z., Raghunathan, S., Verduijn, E., Wood, O., Mangat, P., Goldberg, K., Benk, M., Wojdyla, A., Philipsen, V., et al., "A method of image-based aberration metrology for EUVL tools," Proc. SPIE 9422, 942215–942215 (2015).

[12] Smith, B. W., "Method for aberration detection and measurement," *US Patent* **US7136143 B2** (2006).

[13] Fenger, G. L., Sun, L., Raghunathan, S., Wood, O. R.., Smith, B. W., "Extreme ultraviolet lithography resist-based aberration metrology," J. MicroNanolithography MEMS MOEMS **12**(4), 043001–043001 (2013).

[14] Smith, B. W., "Optics for Photolithography," [Microlithography: Science and Technology], B. W. Smith and K. Suzuki, Eds., CRC Press (2007).

[15] Born, M.., Wolf, E., [Principles of Optics], 7th ed., Press Syndicate of the University of Cambridge (1999).

[16] Nijboer, B., "The Diffraction Theory of Aberrations" (1942).

[17] von Zernike, F., "Beugungstheorie des schneidenver-fahrens und seiner verbesserten form, der phasenkontrastmethode," Publica 1, 689–704 (1934).

[18] Levinson, Z., Burbine, Andrew., Verduijn, E., Wood, O., Mangat, P., Goldberg, K., Benk, M., Wojdyla, A.., Smith, Bruce W., "Image-based pupil plane characterization via principal component analysis for EUVL tools," Proc. SPIE 9776, **977645** (2016).

[19] Manuel Guizar., Efficient subpixel image registration by cross-correlation, MATLAB, http://www.mathworks.com/matlabcentral/fileexchange/18401-efficient-subpixel-image-registration-by-cross-correlation/content/dftregistration.m (2008).

Downloaded From: http://proceedings.spiedigitallibrary.org/ on 03/24/2016 Terms of Use: http://spiedigitallibrary.org/ss/TermsOfUse.aspx